Adaptive Bidirectional Free-Space-Optical Link Resilient to Atmospheric Turbulence

A. Martinez(1), A. Di Tria(1), F. Zanetto(1), F. Morandi(2), A. Milani(2), L. Resteghini(2), F. Morichetti(1), and A. Melloni(1)*

(1) Dipartimento di Elettronica, Informazione e Bioingegneria, Politecnico di Milano, Milan, Italy
(2) Huawei Technologies Italia Srl, Segrate, Italy
Corresponding author: andrea.melloni@polimi.it

Abstract *An adaptive bidirectional Free Space Optical link using programmable optical processors and channel labeling transmits 25Gbit/s OOK signals in an indoor setup, emulating a turbulent link of several hundred meters. ©2025 The Author(s)*

Introduction

Atmospheric turbulence significantly challenges high-bitrate and reliable full-duplex Free Space Optics (FSO) communication systems [1]. To solve these problems, many solutions have been proposed, such as using ultra-short pulse laser (USPL) sources for laser transmission, multi-beam transmission, structured light and orbital angular momentum beams, adaptive optics and broadband transmission systems, hybrid systems, and multi-beam transmission with a beacon [2].

In this work, we implement an adaptive FSO bidirectional communication channel resilient to atmospheric turbulence. Two bidirectional transceivers are used, each of which is a silicon Photonic Integrated Circuit (PIC) comprising an Optical Antenna Array (OAA) controlled by a Programmable Optical Processor (POP). The proposed system automatically establishes the FSO link and optimizes operation during end-to-end power coupling. To this aim, a control strategy based on channel labeling with low-frequency pilot tone modulation is applied to the transmitted signals, thus enabling wavelength reuse in both directions without any impairment. Challenges from parasitic back reflections in PICs are addressed, and solutions are described. Experimental results demonstrate the effectiveness of the proposed approach on high data rate signals (25 Gbit/s OOK) in realistic turbulence conditions.

Bidirectional FSO system implementation: challenges and solutions

Figure 1(a) shows the concept scheme of an FSO transmission system, where a reconfigurable PIC integrates the transmitter and receiver. The waveguide layer of the PIC layout is shown in Figure 1(b), and its components are highlighted. The PIC includes an OAA, made of 16 grating couplers (GCs), and a POP, made of a binary tree of thermally tunable Mach-Zehnder interferometers (MZIs), which acts as a photonic coherent combiner. The PIC can be controlled and reconfigured in real-time to transmit and receive the FSO beam while compensating for the scintillation and wandering caused by atmospheric turbulence [3].

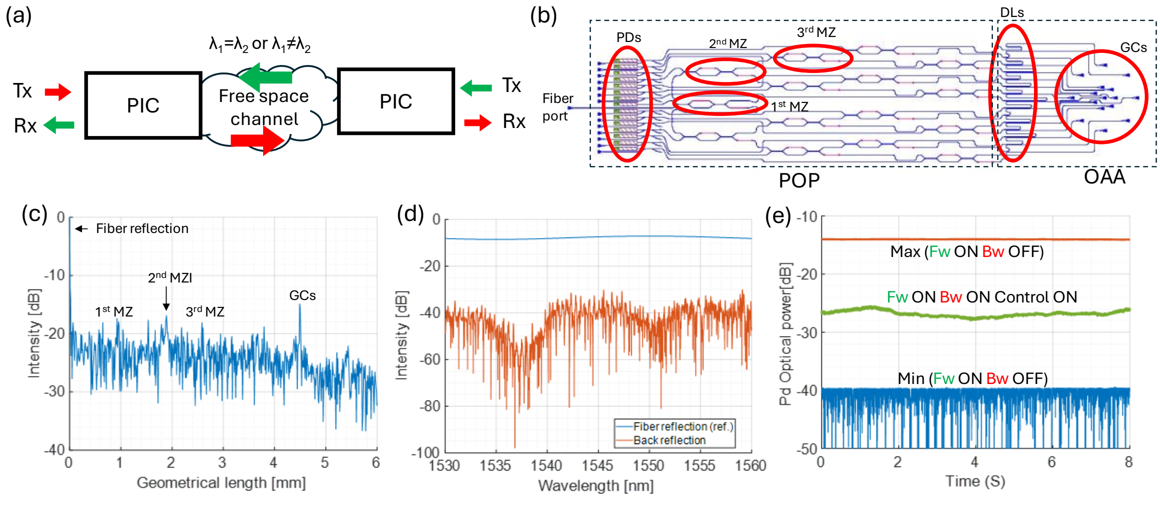

Fig. 1: (a) Schematic of the PIC-to-PIC bidirectional FSO system. (b) Layout of the PIC, including POP and OAA. (c) Backscattering vs Geometrical length of the PIC. (d) Fiber reference reflection (blue curve) and back reflection spectrum of the PIC (red). (e) Received optical power of the last stage monitoring PD for different control conditions.

2025 European Conference on Optical Communications (ECOC) | 979-8-3315-9531-9/25/$31.00 ©2025 IEEE | DOI: 10.1109/ECOC66593.2025.11262956

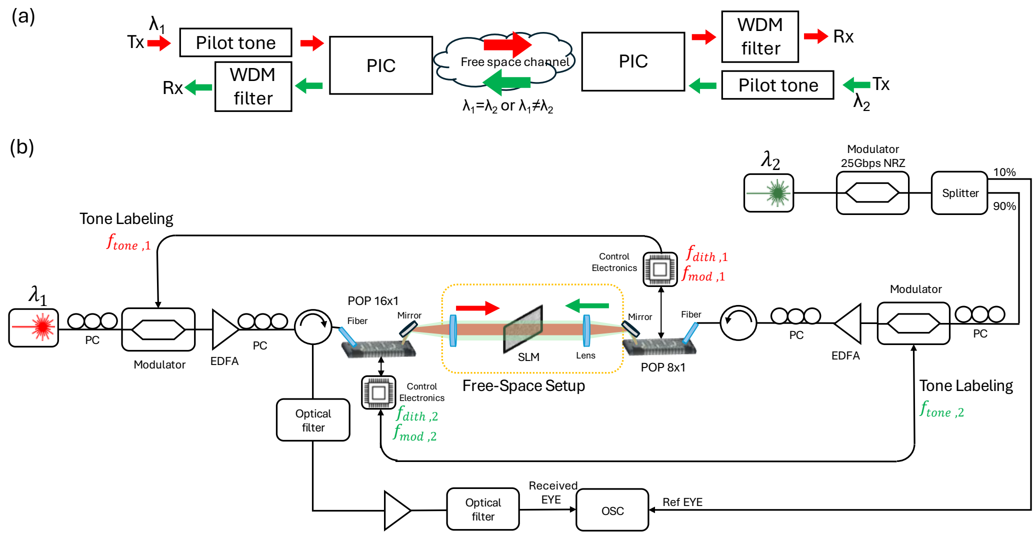

Fig. 2: (a) Block diagram of the full duplex PIC-to-PIC FSO communication system with pilot tone and WDM filters; (b) PIC-to-PIC bidirectional setup experiment schematic. Erbium-doped fiber amplifier (EDFA), Polarization controller (PC), Spatial light modulator (SLM). Real-time oscilloscope (OSC).

The main drawback of implementing a bidirectional link where the two channels share the same physical path comes from parasitic back reflections of the transmitted signal (Tx). In PICs, back reflections originate from the roughness of the WGs, bends, crossings, and GCs [4]. If the back reflected power is higher than the received power, the control system described in [3] won't work correctly. To quantify back reflections in our PICs, we employed the coherent optical frequency domain reflectometry (OFDR) technique to identify critical points where main reflections occur.

Figure 1(c) shows the normalized back reflection of the PIC as a function of the geometrical length along the PIC. The highest reflection ($L = 0$ mm) corresponds to the reference fiber-to-air interface. Then, some peaks are visible, which belong to the reflections caused by the 1st, 2nd, and 3rd MZI stage of the POP and by the GCs of the OAA (the latter resulting in a single peak because all the paths along the POP share the same length). Quantitatively, the highest contribution to the overall back reflection is caused by the GCs.

Figure 1(d) shows the power spectrum of the reference fiber reflection and the PIC back reflection. The total normalized backscattered power P_{bx} equals

$$P_{bx} = P_{bs} + 2L_{loop} - R_{ref} = 23 \text{ dB}, \quad (1)$$

where P_{bs} is the mean power of the back reflections, L_{loop} is the on-chip round-trip loss (around 6 dB), and R_{ref} is the reference fiber reflection. This limits the power margin for the received optical power P_{rx} , which must be at most 23 dB lower than the transmitted power P_{tx} in a bidirectional PIC-to-PIC communication link for the system to work correctly. Such back reflection is an issue for the control system compensating for atmospheric turbulence based on the minimization (or maximization) of monitor PDs integrated into the PICs [3]. Figure 1(e) shows the power of one of the integrated PDs received. The orange (maximum) and blue (minimum) curves show the dynamic range of the PD signals, as is the ideal case (or unidirectional system) in which $P_{bx} = 0$ dB. The green curve shows the reduction of the PD dynamic range due to back reflections when the PIC is also used as a transmitter. In such conditions, the control cannot minimize the PD's power as the optical power of the back reflections is too high, and the received power from the back reflections cannot be discriminated against.

To address this problem, we propose that each PIC transmitter applies a weak intensity modulation to the transmitted signal (pilot tone) [see Fig. 2(a)] with a slow frequency f_{tone} [5]. A low modulation index $\mu < 8\%$ is used to avoid any degradation of the signals. On the Rx side, the control algorithm uses the dithering technique to minimize the PDs readout to compensate for the scintillation [3]. By adding the pilot tone, the complexity of the received spectrum increases as intermodulation components appear at $f_{mod} = f_{dith} \pm (f_{dith} - f_{tone})$. In this case, to minimize the optical power received by the integrated PDs, the control algorithm must zero the intermodulation component (not the dithering signal) [5]. In this way, the received signal can be identified from the transmitted one (even if sharing the same wavelength), regardless of parasitic back reflections. The sensitivity of the label measurement increases with both the modulation depth and the reduction of the electrical bandwidth of the

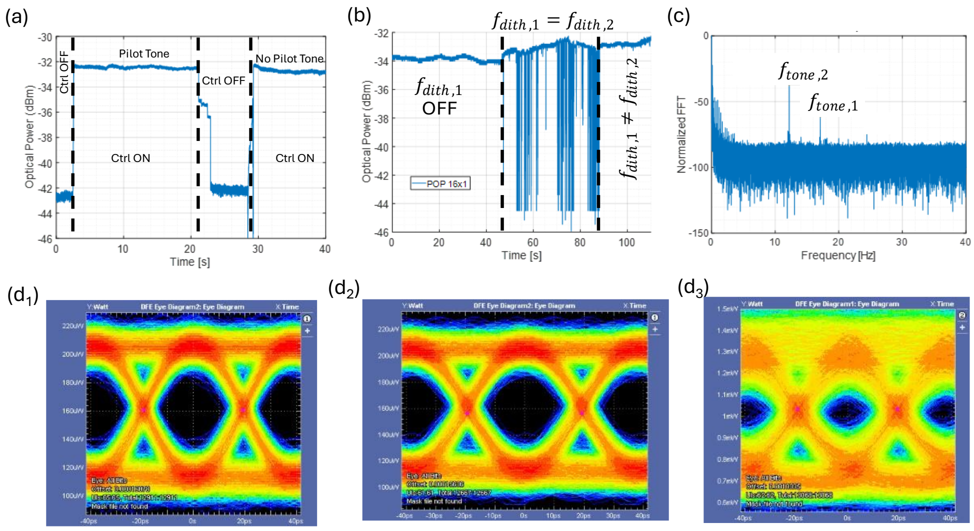

Fig. 3: (a) Received optical power at the left PIC (16x1) with pilot tone, and without pilot tone. (b) Received optical power at the left PIC (16x1) when the control is ON with $f_{dith,1}$ OFF, $f_{dith,1} = f_{dith,2}$, and $f_{dith,1} \neq f_{dith,2}$; (c) Normalized electrical spectrum of the received signal with control ON; Eye diagram of the received 25Gb/s signal after FSO propagation: (d_1) reference, (d_2) P_{rx} is higher than P_{bx}, and (d_3) P_{rx} is 30 dB lower than P_{bx}.

measurement [5].

Experimental Results

To demonstrate the performance of the adaptive bidirectional PIC-to-PIC FSO link, we built the indoor lab setup shown in Fig. 2(b), which is operated at a data rate of 25 Gbps OOK. Realistic turbulence conditions in the FSO link are emulated with a spatial light modulator (SLM) [3]. Figure 3(a) shows the optical power received by the left POP (16x1) when used only as a receiver (unidirectional link): when the control is OFF, the link is not kept aligned, and the received power is around -43 dBm; when the control is activated, the system self establishes and the received power increases up to -32 dBm. Notably, the control of the unidirectional link with and without channel labeling shows the same performance; this means that a shallow pilot tone is not detrimental to the quality of the signal, as confirmed by the received eye diagram in Fig. 3(d_2), with respect to the transmitted (reference) eye of Fig. 3(d_1). When the bidirectional link is activated (left PIC starts transmitting), the system may not work correctly anymore. First, the right-side PIC must use a different dithering frequency or, as shown in Fig. 3(b), the locking condition may be lost (this is because the $f_{dith,1}$ propagates through the FSO channel and interferes with $f_{dith,2}$). When the POP control works well, the intermodulation frequency is absent, and only the two pilot tones are visible in the electrical spectrum of Fig. 3(c). Second, if the received signal is very weak and the back-reflected power is much higher than the received signal, a higher modulation index of the pilot tone is required to keep the system locked. This situation is expected in an FSO link of hundreds of meters, where the channel loss can be very high. This condition is well emulated in our setup, where due to the geometrical losses in the coupling with the OAAs, the total received power is 39 dB lower than that transmitted (+ 7 dBm). Results in Fig. 3(d_3) show the received eye diagram when the received power is 30 dB lower than the back-reflected power. Even in these extreme conditions, pilot tones enable the system to work with partial eye diagram closure (due to the high pilot tone modulation). Solutions to improve the power margin between P_{rx} and P_{bx} include using wavelength-selective filters in front of the integrated PDs and using microlenses on top of the GCs to reduce the geometrical loss and improve the fill factor.

Acknowledgements

This work was supported by the Italian National Recovery and Resilience Plan (NRRP) of NextGenerationEU, partnership on "Telecommunications of the Future" (PE00000001 - program "RESTART", Structural Project "Rigoletto" and Focused Project "Hepic"). The research has been carried out in the framework of the Huawei-Politecnico di Milano Joint Research Lab. Part of this work was carried out at Polifab, the micro- and nanofabrication facility of Politecnico di Milano (https://www.polifab.polimi.it/).

References

[1] Y. Wang, H. Xu, D. Li et al., "Performance analysis of an adaptive optics system for free-space optics communication through atmospheric turbulence." *Scientific Reports* 8, 1124 (2018). https://doi.org/10.1038/s41598-018-19559-9

[2] D. McDonald, R. Bellossi, S. Gladysz, " Field Demonstration of Turbulence-Resilient Coherent Free-Space

Optical Communications Over an 800 m Link," in *European Conference on Optical Communication (ECOC) 2024*, paper M3C.2.

[3] Martinez, A.I., Cavicchioli, G., Seyedinnavadeh, S. et al. "Self-adaptive integrated photonic receiver for turbulence compensation in free space optical links". *Scientific Reports* 14, 20178 (2024). https://doi.org/10.1038/s41598-024-70726-7

[4] D. Melati, A. Melloni, and F. Morichetti, "Real photonic waveguides: guiding light through imperfections," *Advances in Optics and Photonics*. 6, 156-224 (2014). https://doi.org/10.1364/AOP.6.000156

[5] D. O. M. de Aguiar et al., "Automatic Tuning of Silicon Photonics Microring Filter Array for Hitless Reconfigurable Add–Drop," in *Journal of Lightwave Technology*, vol. 37, no. 16, pp. 3939-3947, 15 Aug.15, 2019. DOI: 10.1109/JLT.2019.2916473